

Developing off-design model of Yazd integrated solar combined cycle for analyzing environmental benefits of using solar energy instead of supplementary firing

Authors

Bagher Shahbazi^a
Faramarz Talati^a
S.Mohammad Seyyed Mahmoudi^a
Mortaza Yari^a

^aFaculty of Mechanical Engineering, University of Tabriz, Tabriz, Iran

ABSTRACT

An integrated solar combined cycle (ISCC) is analyzed at "off-design" operating conditions. Using the principles of thermodynamics heat and mass transfer a computer code is developed in FORTRAN programming language to simulate the system's hourly performance under steady state conditions. Three scenarios are considered for the study. In the first one, only the combined cycle (CC) is studied. In the second scenario, two solar heat exchangers are added to the system (ISCC) to produce some extra steam fed to the steam turbine for more power production. In the third one, as that of the ISCC scenario, a supplementary firing is used instead of solar heat exchangers to produce the same power. The main performance parameters are calculated for the hourly variation of solar direct normal irradiation intensity (DNI) and ambient air temperature for analyzing environmental benefits of using solar energy instead of supplementary firing. Results show that the contribution of solar energy in the annual produced power by the ISCC scenario is 75.14 GWh, which is 2.1% of the whole. In addition, it is found that using solar energy leads to an annual reduction of 36.13 Kton in the produced CO₂ and an annual fuel saving of 3.76 ton.

Article history:

Received :20 April 2018

Accepted : 19 August 2018

Keywords: Integrated Solar Combined Cycle, Solar Energy, Off-Design Model, Supplementary Firing, Environmental Benefits.

1. Introduction

In recent years, successful integration of the solar cycle into combined cycle has been reported in several countries such as North Africa, Iran, Italy, Canada and the United

States [1]. According to official statistics, the most solar system production and the largest share of the total power are reported 75 MW and 33.8% for Martin Next Generation Solar Energy Centre power plants in the U.S. and Borges Thermo solar plants in Spain, respectively [1-5]. In these power plants, the desired results achieved from energy and

* Corresponding author: Bagher Shahbazi
Faculty of Mechanical Engineering, University of Tabriz,
Tabriz, Iran
Email: baghershahbazi@gmail.com

economic points of view expressed as increased thermal efficiency and decreased investment funds, have urged abovementioned countries to plan to build them [1],[7]. Other convincing reasons for being absolutely determined to generate ISCCs could be explained as: 1) Repowering power plants complied with environmental laws, 2) Increasing the productivity as well as decreasing greenhouse gas emissions, 3) Reducing the risks related to the construction of large solar projects [8]. In some cases, to be able to use the advantages of these ISCCs such as sustainability, decrease in costs and increase in power and efficiency, the potentiality of the integration of the existing combined cycle power plants with solar energy has been investigated. For example, in [8], the capabilities of the integration solar combined cycle with minimal changes in combined cycle power plant design have been studied for an available combined cycle with a capacity of 390 MW, and the results have led to a change in heating surfaces in the heat recovery steam generator (HRSG).

The optimum compound of solar energy in the combined cycle has been discussed in many papers since the late nineties with the focus on thermodynamic analysis [9]. Kelly et al. [10] demonstrated that the most efficient way for converting solar thermal energy into electricity is to withdraw feedwater from the HRSG downstream of the last economizer, to produce high pressure (HP) saturated steam as well as returning the steam to the HRSG to be superheated and reheated. Rovira et al.[11] came to the same conclusion finding that the highest incremental solar thermal-to-electrical efficiency (44.6%) is achieved when solar heat is used for the evaporation process and eventually for superheating, but not for preheating the feedwater. The ISCC system proposed by Li and Yang [12] wherein both high and low pressure (LP) saturated steam are generated from solar energy, shows an improvement in the thermal match in the HRSG leading to a high solar radiation-to-electric efficiency (up to 30%). Montes et al. [13] considered a 50 MWth hybridization size in a 220 MWel natural gas combined cycle (NGCC) in which preheating and boiling processes take place through collectors and as a result, the increased electricity produced by solar energy compensates for the gas turbine (GT) power drop at high ambient temperatures. [14] showed that the highest thermodynamic

performance is obtained with solar steam generated at the highest temperature and pressure and is fed by upstream HPT. An integration of 80 MWth from CSP into a 200 MWel NGCC with the purpose of comparing different solar power technologies (parabolic trough, linear Fresnel and solar tower) with them was studied by Peterseim et al. [15] Based on various criteria related to feasibility, risk, environmental impact and levelized cost of electricity (LCOE), it was found that Fresnel solar collectors ranked best followed by parabolic troughs using thermal oil as heat transfer fluid. In the study conducted by Aichmayera et al. [16], a 150-megawatt combined cycle power plant was designed using the integration of a solar cycle with combined cycle with the concept of taking energy from the hot air through heat exchangers and providing power by produced steam.

Two criteria for combined cycles including solar cycles are defined as annual ISCC power plant performance optimization and selection of a suitable design point regarding the inherent nature of solar energy; discussed cycles often operate at off-design operating conditions. Since the combined cycle power plants require minimal fluctuations to produce over the years, and an increase in the useful life of components and a decrease in the cost of repairs are obtained due to the reduction in steam turbine (ST) power changes and HRSG steam generated, these power plants should be analyzed during a year at off-design operating conditions, considering that the costs should be reduced.

Researchers have provided a comprehensive description of the design and off-design behavior of ISCCs using commercial softwares (IPSEpro, Thermoflex, GateCycle, Epsilon). Zhu et al. [17] have developed a model of a three pressure level NGCC with solar integration using the IPSEpro software. When solar heat is integrated into the system, the duct burner is turned off to reserve enough capacity room in the ST. They calculated solar thermal-to-electrical efficiencies in the range of 40% to 45% (depending on solar thermal input) which are significantly higher (approximately 10%-points higher) than the steam cycle efficiency. The overall power boost from solar thermal input has reached 83 MWel (from 475 MWel to 558 MWel) which corresponds to a solar share of about 17%. In the evaluation of external heat addition from solar thermal input

at high, intermediate and low pressure HRSG sections in the Thermoflow environment, Gülen [18] observed that HP steam generation increased solar thermal-to-electrical efficiency by 46%. Ojo et al. [19] conducted their integration study based a modern Alstom combined cycle power plant through using a proprietary performance calculation tool. By considering the outlet of condensate pump as feed point to the solar field and the inlet of high pressure turbine (HPT) (560 °C) as solar injection point, boosting power to nearly 70 MWel (up to 15%) was obtained by operating the GT at full load indicating that the swallowing capacity of the HP increased. On the other hand, solar steam can be integrated in operating combined cycles keeping the existing ST and HRSG unchanged. In such conditions, the maximum drum pressure in the HP circuit is gained at 55 MWth solar thermal loads followed by boosting the power output of the combined cycle up to nearly 4.5%. They calculated solar thermal-to-electrical conversion efficiency equal to 35%. Upon studying several configurations for ISCC with collector technologies including parabolic trough, linear Fresnel, and central receiver (power tower), Manente et al. [20] concluded that the most exogetically efficient configuration was parabolic trough one using Therminol VP1 with an efficiency of 61.7%.

In CC power plants, reduction in gas turbine power generation in warm temperatures throughout a year (at high ambient temperature, a diminution in air density decreases both mass flow rate of air and exhaust gas from gas turbine) leads to a fall in HRSG steam production, followed by decreased power generation of the steam turbine (while the steam turbine can get more steam). Supplementary firing in the HRSG could be considered as an effective alternative to compensate for this reduction in power generation. This solution causes a decrease in efficiency as well as an increase in greenhouse gas emissions, heat rate and HRSG gas inlet temperature (for example 560 °C to 580 °C (ambient temperature 40 °C)). This increase in temperature will reduce the life of the pipes and fins in the HRSG. In order to omit the disadvantages of supplementary firing, solar energy and its environmental benefits in a typical power plant (Yazd Combined Cycle Power Plant) are represented in this paper, which can be generalized to the combined cycle power plants with this arrangement. In

this analysis, updated methods with precise details and precision are applied to model each of the main components of studied combined cycle. In addition, the performance of each component and the annual performance of the power plant are discussed through this research.

Nomenclature

A	heat transfer area (m ²)
AC	air compressor
A _f	surface area of a fin (m ²)
A _i	fluid side heat transfer surface (m ²)
A _o	obstruction area (m ²)
A _g	gas side heat transfer surface (m ²)
A _w	average wall surface area (m ²)
BD	blow down
BFP	boiler feedwater pump
CC	combined cycle
COND	condenser
C _p	specific heat capacity (kJ (kg °C) ⁻¹)
CSP	concentrating solar power
DEA	deaerator
d _i	inner diameter of the tube (mm)
DNI	direct normal irradiance (W/m ²)
d _o	outer diameter of the tube (mm)
Eco	economizer
ε _g	gas emissivity
Eva	evaporator
f _i	fouling factor inside tubes
f _o	fouling factor outside tubes
F _T	effectiveness
FTN	Fortran
G	mass flow rate
GT	gas turbine
h _c	average actual outside convective heat transfer coefficient (W.m ⁻² .K ⁻¹)
h _f	fin height (mm)
h _i	average inside heat transfer coefficient (W.m ⁻² .K ⁻¹)
h _N	average outside radiation heat transfer coefficient (W.m ⁻² .K ⁻¹)
h _o	average actual outside heat transfer coefficient (W.m ⁻² .K ⁻¹)
HP	high pressure
HPT	high pressure turbine
HRSG	heat recovery steam generator
HTF	heat transfer fluid
HX	heat exchanger
ISCC	integrated solar combined cycle
K _m	heat transfer coefficient of tube wall (KW (kg °C) ⁻¹)
L	tube length (m)
LCOE	levelized cost of electricity
LMTD	mean-log temperature difference

LP	low pressure
LPT	low pressure turbine
n_f	fin density in tubes (fin m^{-1})
NGCC	natural gas combined cycle
N_w	number of rows wide
P	pressure
SCC	Spencer-Cotton-Canon
SH	super heater
ST	steam control
S_T	transverse pitch, in
t_f	fin thickness (mm)
HX	heat exchanger
ISCC	integrated solar combined cycle
K_m	heat transfer coefficient of tube wall ($\text{KW (kg } ^\circ\text{C)}^{-1}$)
L	tube length (m)

Subscripts

app	approach point
c	convective
cond	conduction
conv	convection
g	gas stream
i	inlet stream
N	nonluminous

o	outlet stream
pp	pinch point
rad	radiation
s	steam stream
sat	saturated
w	water stream

2. System Description

Figure 1 shows a schematic diagram of the cycle. The ISCC in Yazd has a nominal capacity of 474 MW_{el}, and consists of two gas turbines each of them equals to 157 MW_{el} (V94.2 type). The gas turbines are linked with two heat recovery steam generators (HRSG with supplementary firing) supplying steam to a 160 MW_{el} ST. Additional steam is provided by the parabolic mirror field via solar heat exchangers. Hot heat transfer fluid (HTF) is pumped from the parabolic mirror field (LS-3 type [21]) through two heat exchangers where saturated steam is generated. This solar steam is admitted to the HRSGs, and it contributes to an electrical power output of approximately 17 MW_{el} (at rated conditions). Power plant contains a Heller type cooling system.

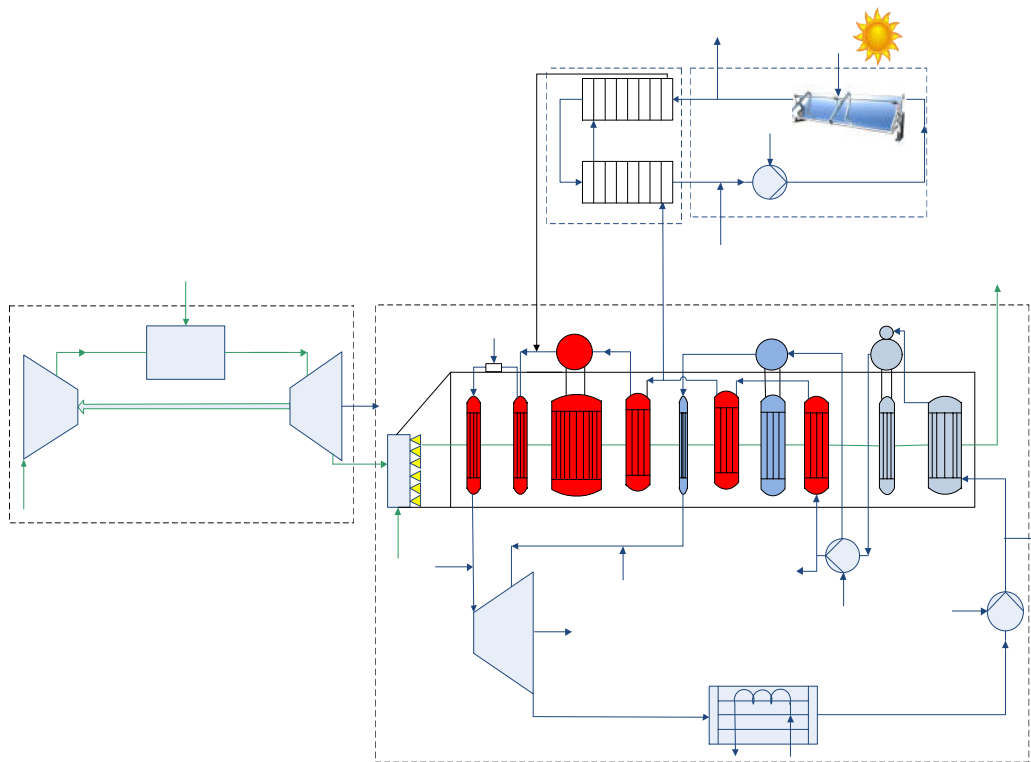


Fig. 1. Schematic diagram of integrated solar combined cycle (ISCCs)

3. ISCC Off-design Modeling

In this section the off-design behavior of the integrated solar combined power plant is analyzed by means of a simulation model developed in the software code (written in FORTRAN programming language). The modeling of main components (gas turbine, HRSG, ST, cooling system and solar field) is expressed. The control philosophy of components used in the off-design conditions is also briefly described. Off-design conditions that intended to analyze the system are variations of environmental conditions (ambient temperature and DNI (Fig.2)).

3.1. Gas Turbine

The thermodynamic design data given under ISO conditions (Table 1) can be approximately converted to other ambient conditions using appropriate correction factors [22]. The correction factors are used for main parameters of GT (power, efficiency, GT outlet temperature, pressure and mass flow rate ...) (Appendix A.1.).

3.2. HRSG

The heat recovery steam generator (HRSG) system produces HP&LP steam of specific quality (correct pressure and temperature) from the thermal energy contained in the GT exhaust gas including supplementary firing and solar heat. Table 1 shows Design data for HRSG cycle (with supplementary firing). For the generation of steam in a Solar Heat Exchanger, a pipe line is considered to extract HP water

from second HP economizer of HRSG and deliver it to the solar heat exchanger. Another pipe line is considered for the delivery of the saturated steam from the Solar Heat Exchanger outlet to HP Steam drum. The geometrical data for all tube banks of the HRSG are included in code to model the real geometry of the HRSG. For each tube bank the energy and heat transfer equations are used (Appendix A.2.). The main steam temperature controller (desuperheater) is considered in off-design modeling that the main task is limiting main steam temperature (max 520 °C). The HRSG load assumed to be 100%, so the diverter damper is fully open.

3.3. Steam Turbine

Determination of multi-stage large ST performance at off-design conditions requires complex numerical calculations. In this paper, to predict the performance of the ST under varying operating conditions the Spencer-Cotton-Canon (SCC) method [23], [24] and the empirical data have been used (Appendix A.3.). The main steam pressure controller is considered in off-design modeling. The ST pressure controller works continuously to meet the main steam pressure set point (72 bar) by the control valves. With increasing steam flow (HRSG load) control valves are opened more and more until at a steam flow of approximately 70% control valves are open 100%. In the upper load range (70...100%) the ST control valves are completely 100% open, so with further increasing boiler load (increasing steam flow) the HP pressure increases too. The design parameters at the ST inlet are shown in Table 2.

Table 1. V94.2 GT stream in ISO conditions

Stream	Pressure (bar)	Temp (°C)	Flow (kg/s)	Gas component (mole %)				
				N ₂	AR	H ₂ O	CO ₂	O ₂
Compressor inlet	1.003	15	495	77.29	0.93	1.01	0.03	20.74
Compressor outlet	11.15	434.2	434.2	77.29	0.93	1.01	0.03	20.74
Turbine inlet	10.88	1148.9	444.1	74.96	0.9	7.1	3.25	13.79
Turbine outlet	1.042	543	504.9	74.96	0.9	7.1	3.25	13.79
Fuel	15.75	25	9.89					

Table 2. HRSG and ST Stream conditions

Equipment	Section	Flow (kg/s)	Pressure (bar)	Temperature (°C)
HRSG	HP	134	95.1	520
	LP	18	9	235
ST	HP	134	90	520
	LP	18	8.5	235

3.4. Cooling System

The turbine exhaust steam is condensed in the direct contact jet condenser by the cooling water. The warmed up water is delivered to the cooling tower for cooling. The cooling deltas divided into several parallel sectors have the major share in cooling duty, that they are assisted by cells of peak coolers connected with them in parallel. The cooling deltas are equipped with louvers on the air inlet side. The louvers are fully opened normally. The peak cooler sectors normally take part in the cooling operation by means of the tower natural draft and there is a seasonal, mechanical draft operation mode. The heat exchangers of the peak cooler cells are deluged in order to enhance cooling capacity in the hottest peak periods (summer). For cooling system modeling, energy and heat and mass transfer equations are used (Appendix A.4.).

3.5. Solar Field

The solar field in Yazd site (Table 3) consists of parabolic trough collectors tracking the sun. Table 3 shows the 'LS-3' collector Specification (design parameters). Heat transfer fluid (HTF (Therminol VP1)) is heated

in the solar field then HTF flow is equally split and pumped through 2 solar heat exchangers each of which consists of an economizer and an evaporator to produce steam. The main control variables are temperature and pressure of the steam leaving the solar steam generator so the temperature of the HTF at the inlet of the heat exchangers is kept constant by adjusting the HTF mass flow rate accordingly via the variable speed HTF pumps. The water level in the evaporator is controlled via an inlet valve located between the HRSG and the solar pre-heater (upstream). The governing equations used in the model of the solar system are presented in (Appendix A.5.). The Table 4 shows the streams condition of solar heat exchanger.

4. Validation

The generated models are validated towards the design base loads and the off-design operations (CC reference, different solar load, supplementary firing) the obtained results for main outputs show good agreement with the real data. For validation of the model, the real and practical data and the documents of the Yazd power plant have been used. Table 5 shows the validation of model in different scenarios.

Table 3. Geographical coordinate and collector specification of the solar site

Geographical coordinate		
Altitude [m as]	Longitude [$^{\circ}$]	Latitude [$^{\circ}$]
1100	54.042	31.939
Collector Specification		
Aperture area per SCA	m ²	545
Number of collector	-	216
Total collector area of solar field	m ²	104640
HCE absorptivity	%	0.96
HCE emittance	-	0.17
HCE transmittance	-	0.96
Peak collector efficiency	%	0.68
Mirror reflectivity	-	0.94
Optical efficiency	%	80

Table 4. Solar preheater and evaporator streams condition

Feed water inlet to HE: Temp (°C)	210
Feed water inlet to HE: Pres (bar)	116
Steam outlet from HE: Temp (°C)	310
Steam outlet from HE: Pres (bar)	98
Steam flow rate (kg/s)	13.1
HTF inlet Temp (°C)	392
HTF inlet Pres (bar)	16
HTF outlet Temp (°C)	299
HTF outlet Pres (bar)	11
HTF flow rate (kg/s)	109

Table 5. Validation of the model results with real data

a. Ambient Temperature = 19 (°C) & Without Solar & Duct Burner Fuel = 0.74 kg/s									
	Flow(kg/s)			Temperature (°C)			Pressure (bar)		
	Real	Model	Error	Real	Model	Error	Real	Model	Error
GT Exhaust	429	429.9	0.21	548	544.9	0.57	-	-	-
HP Steam	67.07	65.63	2.15	523	520	0.57	95.2	94.8	0.42
LP Steam	9	9.5	5.5	234	233.8	0.09	9.6	9.7	1.04
STG Output	151.66	150.9	0.50	47.2	46.47	1.55	0.112	0.11	1.8
Condenser Output	152.17	150.9	0.83	47.2	46.47	1.55	0.112	0.11	1.8
Stack Out	430.04	430.6	0.13	113	109	3.54	-	-	-
Steam turbine Power Output (MW)	Real (160.4)	Model (157.6)	Error (1.75 %)						

b. Ambient Temperature = 19 (°C) & Solar (100%) 800 W/m² & Duct Burner Fuel = 0.225 kg/s									
	Flow(kg/s)			Temperature (°C)			Pressure (bar)		
	Real	Model	Error	Real	Model	Error	Real	Model	Error
GT Exhaust	429	429.9	0.21	548	544.9	0.57	-	-	-
HP Steam	67.07	65.96	1.65	523	520.1	0.55	95.2	94.8	0.42
LP Steam	9.5	9.87	3.8	235	235	0.0	9.6	9.69	0.94
STG Output	151.66	151.5	0.11	47.2	48.07	1.84	0.112	0.11	1.8
Condenser Output	152.17	151.5	0.11	47.2	48.07	1.84	0.112	0.11	1.8
Stack Out	429.525	430.1	0.13	113	113.7	0.62	-	-	-
HTF Inlet Filed	218	216.9	0.50	299	298.5	0.17	16	16	0.0
HTF Outlet Filed	218	216.9	0.5	392	392	0.0	11	10.5	4.5
Water inlet Solar Heat Exchanger	13.1	13.02	0.6	210	212	0.96	116	114.7	1.12
Steam Outlet Solar Heat Exchanger	13.1	13.02	0.6	310	313.7	1.19	98	102	4.0
Steam turbine Power Output (MW)	Real (160.4)	Model (158.5)	Error (1.18 %)						

5. Results and Discussion

In this paper, a comprehensive code of ISCCs cycle modeling is developed (zero-dimensional models for each component in the gas and steam cycle and solar field are developed in FTN programming language). The important points in this modeling could be expressed as follows:

- A zero-dimensional model for each component in the gas and steam cycle and solar field is developed.
- Details of the cycle (such as desuperheater, vent steam flow, blowdown flow, etc.) and the control philosophy of the main components are considered.
- The results obtained from the model are validated in different scenarios with real data.
- The annual performance of the power plant has been studied with considering the changes in the two environmental parameters (temperature and DNI).

- The environmental benefits of using solar energy instead of supplementary firing have been investigated.

A sensitivity analysis is applied in order to investigate the variations of output parameters of the main components and power plant by taking changes forced on some input parameters into consideration. Table 6 shows the composition of fuel used in gas turbines and burners.

Table 6. Natural gas composition

Component	Volume (%)	LHV (kJ/kg)
CH ₄	88.17	50047
C ₂ H ₆	3.91	47525
C ₃ H ₈	1.2	46390
C ₄ H ₁₀	0.58	45769
C ₅ H ₁₂	0.24	45400
N ₂	5.38	-
CO ₂	0.07	-
Others	0.45	-
Total	100	45264

- Gas Turbine

Due to the reduction in the air density and regarding the constant volumetric flow rate at the compressor inlet which is resulted from constant rotor speed, the mass flow rate of air and exhaust gases decrease at high ambient temperatures. The control system holds turbine inlet temperature (TIT) constant, consideration of this fact coupled with the constant corrected mass flow in gas turbine leads to a decrease in pressure ratio and air mass flow rate which is indicated in Fig.3 (a). Variation of the power and efficiency due to the change of ambient temperature is shown in Fig. 3 (b). A reduction in exhaust gases mass flow rate and pressure ratio causes a decrease in GT power output and a reduction in the net specific work decreases thermal efficiency too.

- HRSG

A reduction in the HP and LP steam flow rate and pressure caused by a decrease in GT exhaust gases mass flow rate (GT part load) are demonstrated in Fig.4 (a) and Fig.4 (b) respectively. Due to the reduction in overall heat transfer coefficient and minimum temperature differences at reduced load, the heat duty of each heat exchanger decreases compared to the nominal heat duty.

- Steam Turbine

With decreasing ST inlet steam Mass flow rate and pressure (pressure ratio) the turbine isentropic efficiency decreases. Accordingly, the power generation of HPT and low pressure turbine (LPT) decrease at reduced load. Fig.5 (a) and (b) shows the variation of HPT and LPT and total ST power generation with GT part load and ambient temperature.

- Cooling System

Figure6 shows the variation of condenser pressure due to ambient temperature rise. The minimum back pressure (control choking point) and condenser pressure at site condition (design point 19 °C) are 0.084 bar and 0.112 bar respectively (the best back pressure for ST). With increasing ambient temperature condenser pressure increases. Peak coolers are used in summer and peak cooler cells are deluged at the hottest peak periods ($T > 32$ °C). The effect of condenser pressure on ST performance is also shown in Fig.6.

- Solar Field

Solar irradiation (DNI), the difference between operating temperature and ambient temperature and solar position, which is a function of solar azimuth and solar elevation and thus a function of time, cause variations in the efficiency of solar collectors. The thermal efficiency curve for the solar collector is shown in Fig.7. In the case of decreasing DNI to hold the HTF outlet temperature constant, HTF mass flow rate decreases by variable speed HTF pumps. Fig.8 (a) shows slight variations HTF inlet temperature and variation of solar steam generation caused by reduction of HTF mass flow rate is indicated in Fig.8 (b).

- ISCC

The ISCC generated electricity depends mainly on the ambient temperature and direct normal irradiance. Figure 9 shows the changes in the ISCC main outputs including electrical power generation, fuel consumption, efficiency and heat rate in different cases of operation. These cases contain different ambient temperature (site condition (19 °C), max site winter condition (-4 °C), max site summer condition (46 °C) ...) and different operation scenarios (case1: ref CC. case2: CC 100% & solar 0%. case3: CC 100%, solar 0% & supplementary firing fuel 0.225 kg/s. case4: CC 100%, solar 25%. Case5: CC 100%, solar 50%. Case6: CC 100%, solar 75%. Case7: CC 100%, solar 100%. Case8: CC 90%, solar 120%). Results show the CC regarding supplementary firing case has minimum efficiency, Maximum heat rate and maximum fuel consumption, and when the solar load is maximum (120%) fuel consumption and heat rate are minimum and efficiency is maximum.

- Annual Performance

The hourly performance values of the ISCC have been calculated for the hourly values of solar irradiation (DNI) and the hourly ambient air temperature for the average year and three scenarios are considered to analyze the environmental benefits and fuel saving operation of ISCC: 1- the ISCC is assumed to be operated at full GT power, without supplementary firing and using the available solar heat. 2-the reference combined cycle (CC without the solar field and without supplementary firing). 3-the reference CC (without the solar field) with use of

supplementary firing (the control loop is defined in model to control the mas flow rate of duct burners to produce electricity power equal to the power generated in the ISCC mode). Figure 10 (a) demonstrates the comparison between monthly energy production of the ref CC and ISCC and the

monthly solar incremental energy production of ISCC could be seen in Fig.10 (b) . Results (Fig. 10 and Fig.11) show that the annual solar generation of ISCC, reduction of CO₂ due to solar generation and annual fuel saving are 75.14 GWh, 36.13 Kton and 3.76 ton respectively.

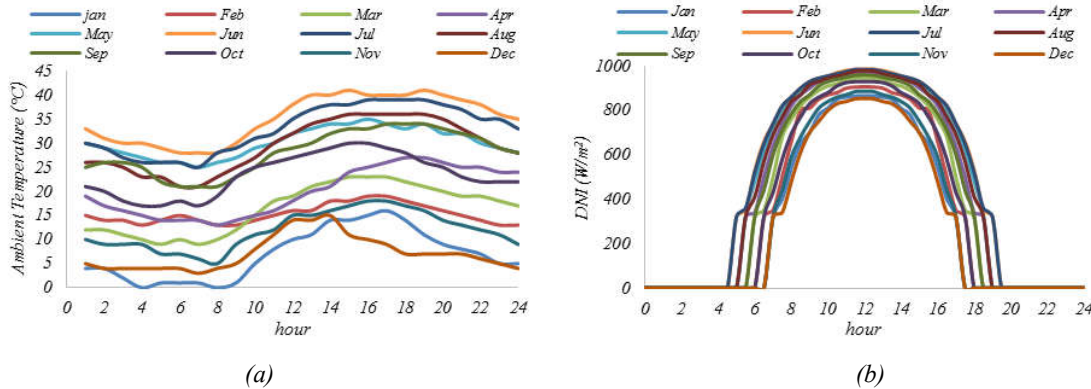


Fig. 2. (a) Hourly monthly mean of ambient air temperature: (b) Hourly monthly mean of DNI (satellite readings for Yazd)

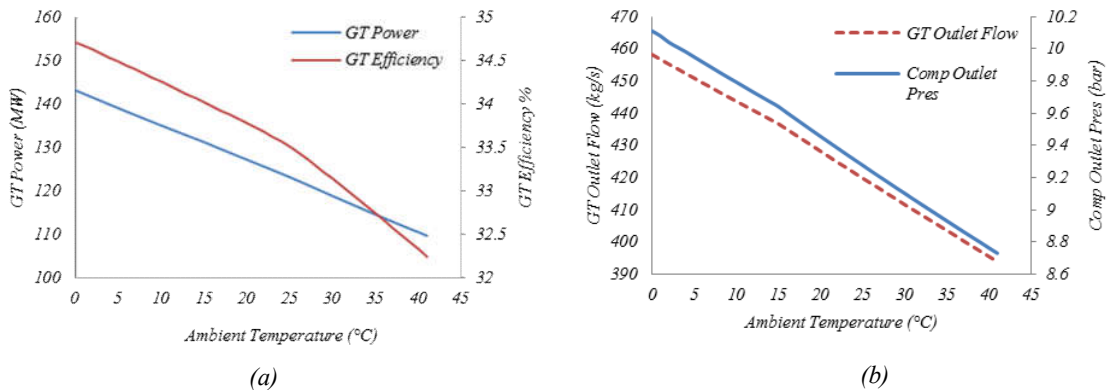


Fig. 3. (a) Variation of GT power and efficiency with ambient temperature: (b) Variation of GT outlet flow rate and compressor outlet pressure with ambient temperature

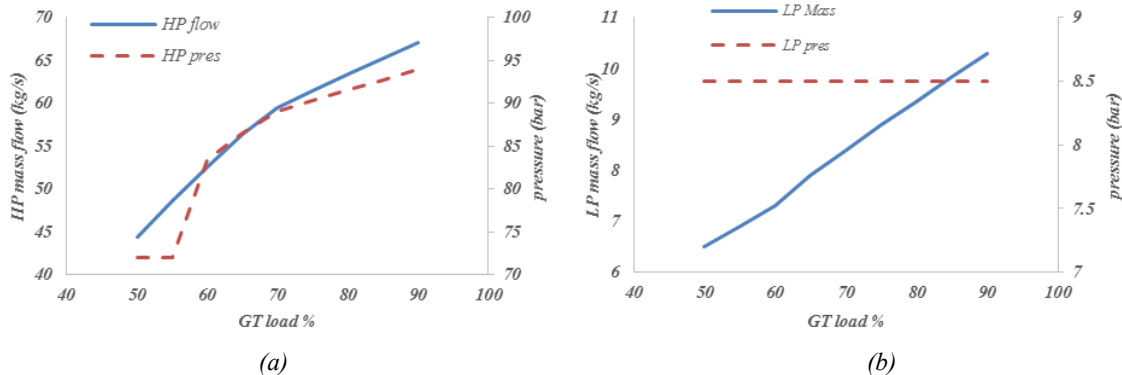


Fig. 4. (a) Variation of HP steam flow and pressure with GT load: (b) Variation of LP steam flow and pressure with GT load

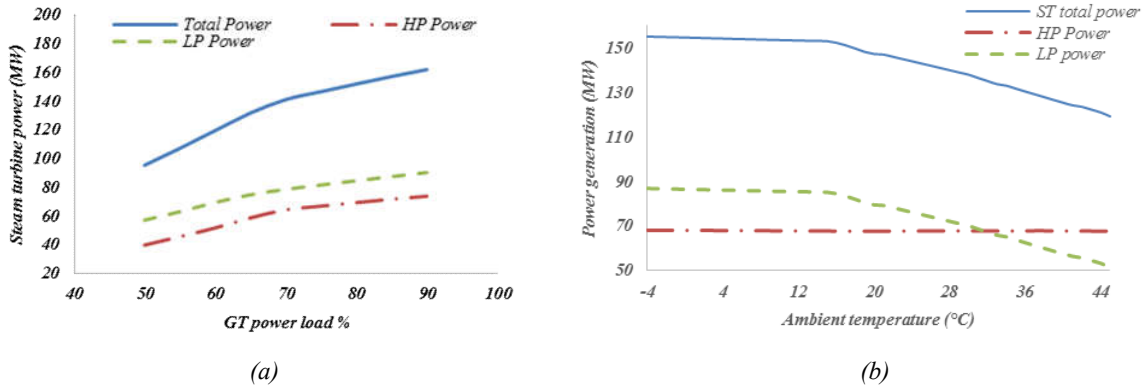


Fig. 5. Variation of HPT and LPT and total ST power generation with a) GT load: (b) ambient temperature

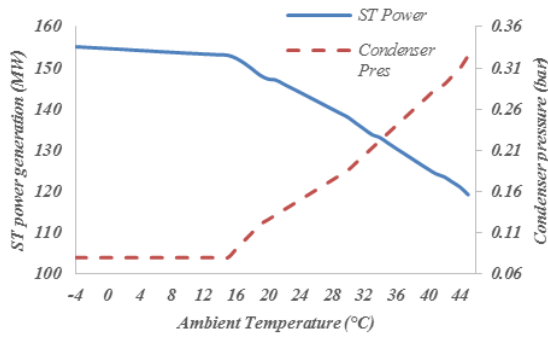


Fig. 6. Variation of condenser pressure and ST power generation with ambient temperature

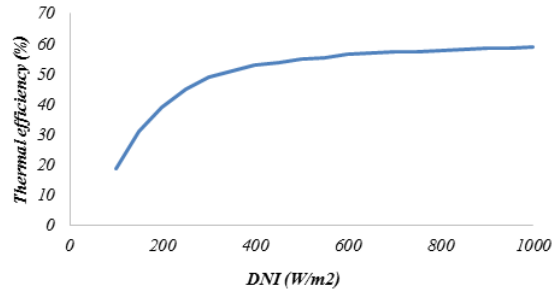


Fig. 7. Thermal efficiency of solar collector

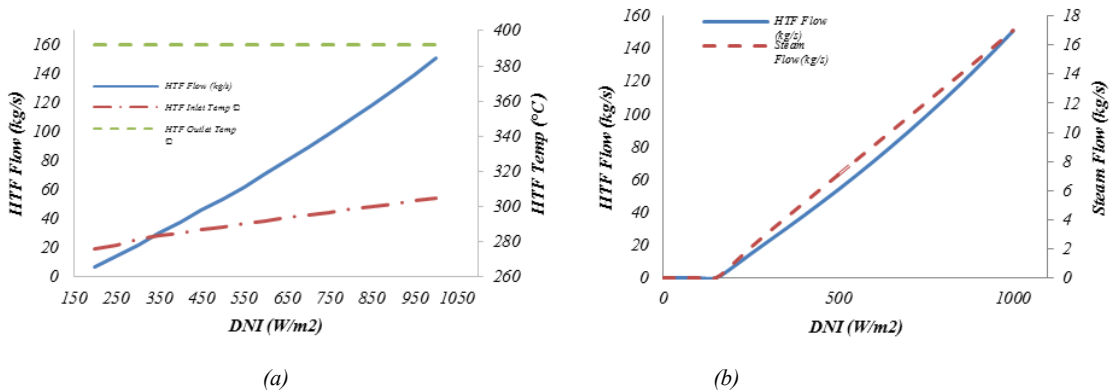


Fig. 8. (a) Variation of HTF flow rate and inlet and outlet temperature with DNI: (b) Variation of HTF flow rate and solar steam flow rate with DNI

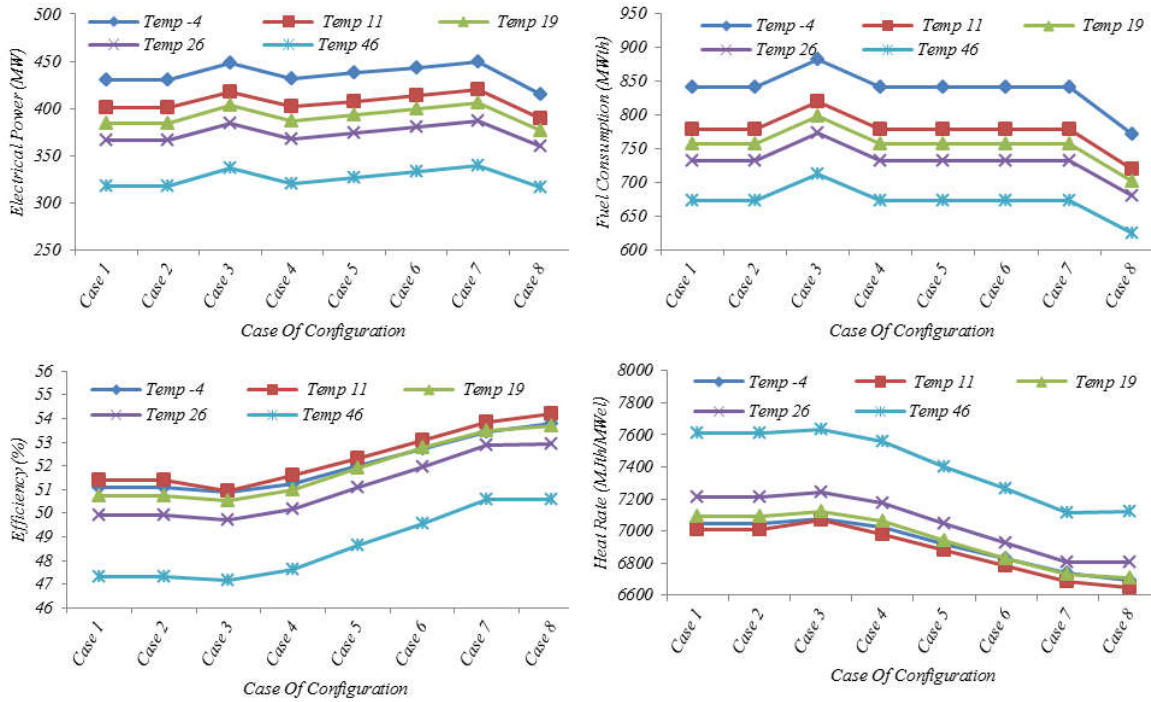


Fig. 9. The ISCC Electrical power generation, fuel consumption, efficiency and heat rate in different scenarios of operation

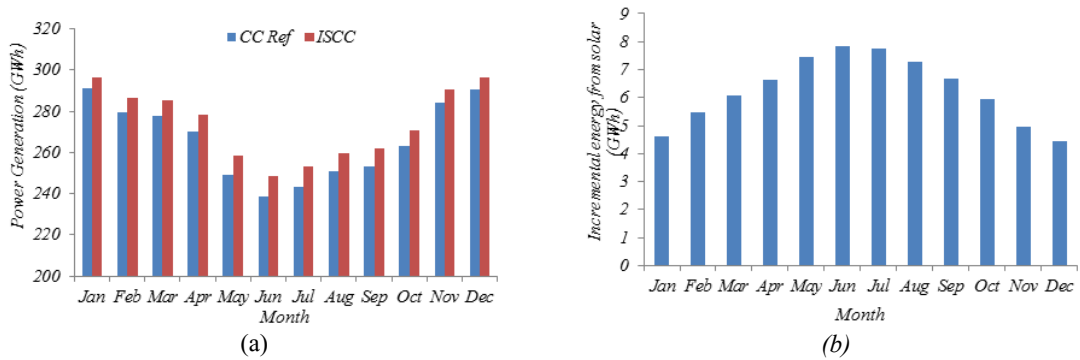


Fig. 10. (a). Monthly power generation of ISCC and CC reference (b). monthly solar incremental energy production of ISCC

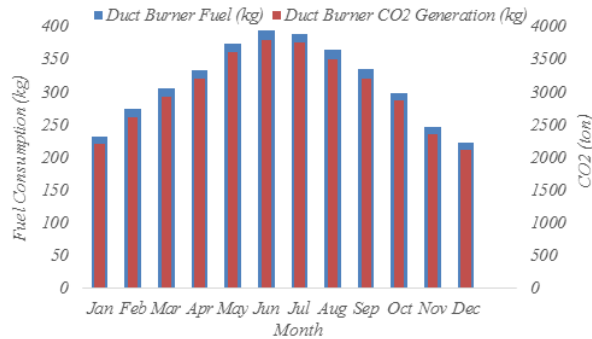


Fig. 11. Monthly fuel consumption and CO₂ production of ISCC

6. Conclusion

Depletion of fossil fuels and global warming accelerate activities to improve use of renewable energy (especially solar energy). The integrated solar combined cycle system (ISCCS) is one of the more promising hybrid configurations for converting solar energy into electricity. In the present paper, the off-design model of integrated solar combined cycle is developed. The main components of the cycle are modeled based on mathematical models that derived from conservation equations for mass, energy and momentum with combined heat transfer coefficient formulations. The values of the GT, HRSG, ST, cooling system and solar field parameters and power output at any ambient conditions with different temperatures and radiations, could be calculated through off-design model. In the case of same electricity generation and reducing greenhouse gas emissions, this model analyzes the performance of the CC reference with solar instead of the CC reference with supplementary firing. Based on the hourly values of solar irradiation and ambient air temperature, the values of hourly ISCC performance are calculated. The key findings from this study can be summarized into the following points:

- According to the results, the power generation of the CC reference without solar part and supplementary firing, efficiency and heat rate are 384.45 MW, 50.75% and 7093.55 MJth/MW_{el} at 19 °C (Design point) respectively while they are 403.45 MW and 53.51 % and 6727.4 MJth/MW_{el} for the ISCC in which solar energy with a irradiation of 800 W/m² is used. It is also investigated that applying supplementary firing instead of solar energy to produce the same power supplied by the ISCC (403.45 MW), results in 50.54 % and 7122.6 MJth/MW_{el} as the values of efficiency and heat rate respectively.
- The contribution of solar energy in the annual produced power by the ISCC is 75.14 GWh which is 2.1% of the total.
- Annual reduction of 36.13 Kton in producing CO₂, the reduction of the social cost of CO₂ emission and annual fuel saving of 3.76 ton could be counted as other benefits of using solar energy.
- Due to the upper limit of steam turbine inlet temperature and heating surfaces temperature in HRSG, some limitations on using of supplementary firing are imposed while

applying solar energy in the hottest peak periods (summer) removes them.

Reference

- [1] Behar O., Khellaf A., Mohammedi K., Ait-Kaci S., A review of Integrated Solar Combined Cycle System (ISCCS) with a Parabolic Trough Technology, *Renewable and Sustainable Energy Reviews* (2014) 39:223–50.
- [2] The World Bank, (<http://www.worldbank.org/en/results/2014/04/15/demonstrating-the-viability-of-solar-thermal-power-in-morocco>) (2014) [accessed 21.09.15].
- [3] Clean Energy Action Project, (<http://www.cleanenergyactionproject.com/>) Clean Energy Action Project/CS. FPL Martin Next Generation Solar Energy Center Hybrid Renewable Energy Systems Case Studies.html (2015) [accessed 23.09.15].
- [4] Archimede Solar Energy Company Presentation. Archimede project, solar receiver tubes and concentrated panels. ([http://www.ceees.org/downloads/tabcap/Archimede CEEES Feb 2009.pdf](http://www.ceees.org/downloads/tabcap/Archimede%20CEEES%20Feb%2009.pdf)); (2015) [accessed 23.09.15].
- [5] SET at Work Good Practice. First Application in the World of the Integration of a Combined Gas Cycle with a Solar Plant, Italy ([http://www.setatwork.eu/downloads/SGP7 CGS Solar IT.pdf](http://www.setatwork.eu/downloads/SGP7%20CGS%20Solar%20IT.pdf)) (2015) [accessed 23.09.15].
- [6] Jamel M.S., Rahman A.A., Shamsuddin A.H., Advances in the Integration of Solar Thermal Energy with Conventional and Non-Conventional power plants, *Renewable and Sustainable Energy Reviews* (2013) 20:71–81.
- [7] Bachmann R., Nielsen H., Warner J., Rolf Kehlhofer, Kehlhofer R., *Combined Cycle Gas & Steam Turbine Power Plants*, 2nd Edition Tulsa, Okla PennWell (1989).
- [8] Giovanni Manente., High Performance Integrated Solar Combined Cycles with Minimum Modifications to the Combined Cycle Power Plant Design, *Energy Conversion and Management* (2016) 111:186–197.
- [9] Allani Y., Favrat D., von Spakovsky MR., CO₂ Mitigation through the Use of Hybrid Solar-Combined Cycles, *Energy*

- Conversion and Management (1997) 38:661–667.
- [10] Kelly B., Herrmann U., Hale M.J., Optimization Studies for Integrated Solar Combined Cycle Systems, International Solar Conference (2001) 1:1-7
- [11] Rovira A., Montes M.J., Varela F., Gil M., Comparison of Heat Transfer Fluid and Direct Steam Generation Technologies for Integrated Solar Combined Cycles, Applied Thermal Engineering (2013) 52:264–74.
- [12] Li Y., Yang Y., Thermodynamic Analysis of a Novel Integrated Solar Combined Cycle, Applied Energy (2014)122:133–42.
- [13] Montes M.J., Rovira A., Muñoz M., Martínez-Val J.M., Performance Analysis of an Integrated Solar Combined Cycle Using Direct Steam Generation in Parabolic trough Collectors, Applied Energy (2011) 88:3228–38.
- [14] Libby C., Golden J., Bedilion R, Turchi C., Assessment of Direct Steam Generation Technologies for Solar Thermal Augmented Steam Cycle applications, Energy Procedia (2014) 49:1420–8.
- [15] Peterseim J.H., White S., Tadros A., Hellwig U., Concentrated Solar Power Hybrid Plants, which Technologies Are Best Suited for Hybridization, Renewable Energy (2013) 57:520–32.
- [16] Aichmayera L., Spellingb J., Laumerta B., Thermoeconomic Analysis of a Solar Dish Micro Gas-turbine Combined-cycle Power Plant, Energy Procedia (2015) 69:1089–1099.
- [17] Zhu G., Neises T., Turchi C., Bedilion R., Thermodynamic Evaluation of Solar Integration into a Natural Gas Combined Cycle Power Plant, Renewable Energy (2015) 74:815–24.
- [18] Gülen S.C., Second Law Analysis of Integrated Solar Combined Cycle Power Plants, Journal of Engineering for Gas Turbines and Power (2015) 137. 051701:1-9.
- [19] Ojo C.O., Pont D., Conte E., Carroni R., Performance Evaluation of an Integrated Solar Combined Cycle. Proceedings of ASME Turbo Expo (2012) 6:261-270.
- [20] Manente G., Rech S., Lazzaretto A., Optimum Choice and Placement of Concentrating Solar Power Technologies in Integrated Solar Combined Cycle Systems, Renewable Energy (2016) 96:172–89.
- [21] Kearney D., Price H., Parabolic-Trough Technology Roadmap a Pathway for Sustained Commercial Development and Deployment of Parabolic-Trough Technology (1999) SunLab NREL.
- [22] Technical Data for Deviations from Design Conditions. Yazd Power Plant Technical Documents.
- [23] Spencer R.C., Cotton K.C., Cannon C.N., A Method for Predicting the Performance of Steam Turbine-Generator Unit 16,500 kW and Larger, Engineering for Power (1963) 85(4):249-298.
- [24] Chacartegui R., Sánchez D., Becerra J.A., Muñoz A., Sánchez T., Performance Analysis of a 565 MW Steam Power Plant, Proceedings of ASME Turbo Expo, (2011) 7: 2427-2436.
- [25] Antonanzas J., Alia-Martinez M., Martínez-de-Pison F.J., Antonanzas-Torres F., Towards the Hybridization of Gas-Fired Power Plants: A Case Study of Algeria, Renewable and Sustainable Energy Reviews (2015) 51:116–24.
- [26] Trad A., Ameziane Ait A.M., Determination of the Optimum Design through Different Funding Scenarios for Future Parabolic trough Solar Power Plant in Algeria, Energy Convers Manage (2015) 91:267–79.
- [27] Naemi S., Saffar-Avvala M., Behboodi Kalhorib S., Mansoori Z., Optimum Design of Dual Pressure Heat Recovery Steam Generator Using Non-Dimensional Parameters Based on Thermodynamic and Thermoeconomic Approaches, Applied Thermal Engineering (2013) 52:371-84.
- [28] Ganjehkaviri A., Mohd Jaafar M.N., Mat Lazim T., Barzegaravval H., Exergoenvironmental Optimization of Heat Recovery Steam Generators in Combined Cycle Power Plant through Energy and Exergy Analysis, Energy Conversion and Management (2013) 67:27-33.
- [29] Ganapathy V., Industrial Boiler and Heat Recovery Steam Generator (2003) ISBN 0-8247-0814-8, Marcel Dekker.

- [30] Kröger D.G., Air-Cooled Heat Exchangers and Cooling Towers (2004) 1, ISBN 1-59370-019-9, PennWell.
- [31] Arsenyeva O., Kapustenko P., Klemeš J., Tovazhnyanskyy J., Leonid-Compact Heat Exchangers for Transfer Intensification Low Grade Heat and Fouling Mitigation (2015) ISBN 0-07-295358-6, CRC.
- [32] Gnielinski V., New Equations for Heat and Mass-Transfer in Turbulent Pipe and Channel Flow, International Chemical Engineering (1976) 16:359-368.
- [33] Incropera F.D., DeWitt, Fundamentals of Heat and Mass Transfer, 8th Edition (2017) ISBN 978-1-119-32042-5, John Wiley and Sons.
- [34] Mokhtari H., Ahmadisedigh H., Ebrahimi I., Comparative 4E Analysis for Solar Desalinated Water Production by Utilizing Organic Fluid and Water, Desalination (2016) 377:108–122.

Appendix A

A.1.) Gas turbine formulation

The following Equation depicts these correction factors as a function of the individual ambient conditions [24].

$$\eta_{GT-CORR} = \eta_{GT1} \times \eta_{GT2} \times \eta_{GT3} \times \eta_{GT4} \times \eta_{GT5} \times \eta_{GT6} \times \eta_{GT7} \times \eta_{GT8} \times \eta_{GT9} \times \eta_{GT10} \quad (A-1)$$

- η_{GT1} Efficiency at generator terminals under ISO conditions
- η_{GT2} Correction factor for intake pressure drop
- η_{GT3} Correction factor for exhaust pressure drop
- η_{GT4} Correction factor for lower heating value
- η_{GT5} Correction factor for humidity
- η_{GT6} Correction factor for speed
- η_{GT7} Correction factor for ambient temperature
- η_{GT8} Correction factor for part load
- η_{GT9} Correction factor for water or steam injection
- η_{GT10} Correction factor for aging

A.2.) HRSG formulation

Energy balance, heat transfer and heat transfer coefficient equations for all heat transfer surfaces between the hot and cold streams (gas side and water/steam side) are listed as fowling:

Burner:

$$m_{g,i} h_{g,i} + \eta_{burner} \cdot m_{fuel} \cdot LHV_{fuel} = (m_{g,i} + m_{fuel}) \cdot h_{g,o} \quad (A-2)$$

Energy balance Equations for HXs

$$m_g C_p g (T_{g,i} - T_{g,o}) = m_s (h_{s,o} - h_{s,i}) + \dot{Q}_{loss} \quad (A-3)$$

Heat Transfer Equation for HXs

$$U \times A \times LMTD = m_g C_p g (T_{g,i} - T_{g,o}) \quad (A-4)$$

$$LMTD = F_T \times \frac{(T_{g,i} - T_{w,o}) - (T_{g,o} - T_{w,i})}{\ln \left(\frac{T_{g,i} - T_{w,o}}{T_{g,o} - T_{w,i}} \right)} \quad (A-5)$$

$$\frac{1}{U} = \frac{1}{\eta_o h_o} + f_o + \frac{A_t}{A_{wi}} f_i + \frac{A_t}{A_{wi}} \frac{1}{h_i} + \frac{A_t}{A_w} \frac{d_o \ln \left(\frac{d_o}{d_i} \right)}{2K_m} \quad (\text{A-6})$$

Heat transfer Surface

$$A_t = A_f + \pi d_o (1 - n_f t_f) \quad (\text{A-7})$$

$$A_f = \pi n_f (2d_o h_f + 2h_f^2 + 2t_f h_f) \quad (\text{A-8})$$

$$A_i = \frac{\pi d_i^2}{4} \quad (\text{A-9})$$

$$A_w = \pi \left(\frac{d_o + d_i}{2} \right) \quad (\text{A-10})$$

Heat Transfer coefficient

Average outside radiation heat transfer coefficient

$$h_N = \sigma \varepsilon_g \frac{T_g^4 - T_o^4}{T_g - T_o} \quad (\text{A-11})$$

$$\varepsilon_g = \varepsilon_{CO_2} + \varepsilon_{H_2O} - \Delta \varepsilon_{Overlap} \quad (\text{A-12})$$

Average actual outside convective heat transfer coefficient

$$h_c = C_3 C_f C_5 \left(\frac{d_o + 2h_f}{d_o} \right)^{0.5} \times \left(\frac{T_g + 273}{T_a + 273} \right)^{0.25} \times GC_p \times \left(\frac{k}{\mu C_p} \right)^{0.67} \quad (\text{A-13})$$

Average actual outside heat transfer coefficient

$$h_o = h_N + h_c \quad (\text{A-14})$$

Average inside heat transfer coefficient economizer and preheater

economizer and preheater:

$$h_i = 0.023 \frac{k}{d_i} Re^{0.8} Pr^{0.4} \quad (\text{A-15})$$

super heater:

$$h_i = 0.0133 \frac{k}{d_i} Re^{0.84} Pr^{1/3} \quad (\text{A-16})$$

evaporator and deaerator:

$$hi_1 = 34.10 \times 44.4 \left(q^{0.5} \right) EXP \left(\frac{P}{86.87} \right) \quad (A-17)$$

$$hi_2 = 184.66 \times 1.266 \left(q^{0.75} \right) EXP \left(\frac{P}{62} \right) \quad (A-18)$$

$$h_i = \max(hi_1, hi_2) \quad (A-19)$$

Fin Efficiency

$$\eta = 1 - (1 - E) \frac{A_f}{A_t} \quad (A-20)$$

Where G is Mass flow rate (kg/h), P is Pressure (absolute bar), d_o and d_i is the outer and inner diameter of pipes, respectively. n_f is the number of fins, t_f is the fin's thickness and h_f is its height, K_m is the thermal conductivity of the tube wall, and f_i and f_o represent fouling factors inside and outside the tubes, h_i and h_o are tube-side and gas-side heat transfer coefficients ($W/m^2 \cdot ^\circ C$). C_1 , C_2 , C_3 are defined in Ref.[31] and μ is viscosity (Pa.s) [21], [27]-[31].

A.3.) Steam turbine

The following equation depicts these correction factors as a function of the inlet steam conditions and ST specifications [23], [24].

$$\eta_{ST-CORR(HP\&LP)} = \eta_{Base-HP} \times (1 - \eta_{ST1}) \times (1 - \eta_{ST2}) \times (1 - \eta_{ST3}) \times (1 - \eta_{ST4}) \times (1 - \eta_{ST5}) \quad (A-21)$$

- η_{Base} Base efficiency
- η_{ST1} efficiency correction for volume flow
- η_{ST2} efficiency correction for governing stage
- η_{ST3} efficiency correction for pressure ratio
- η_{ST4} efficiency correction for initial condition
- η_{ST5} efficiency correction for governing stage at part load

The following Losses are considered for obtaining output power.

- Exhaust loss
- Packing and valves leakage losses
- Mechanical loss
- Generator loss

A.4.) cooling system formulation

Energy balance equations (between steam and condenser cooling water and the air stream):

$$\dot{Q} = \dot{m}_s (h_{in} - h_{out}) = \dot{m}_w C p_w (T_{w,o,c} - T_{w,in,c}) = \dot{m}_a C p_a (T_{a,o,H} - T_{a,i,H}) \quad (A-22)$$

Heat transfer equation:

$$\dot{Q} = F_r U . A . \Delta T_{Log} \quad (A-23)$$

Heat transfer surface:

$$A_p = \pi d_o (L_1 - t_f N_f L_1) N_t \quad (A-24)$$

$$A_f = 2 \left[\frac{L_2 L_3 - \pi d_o^2 N_f}{4} \right] N_f L_1 + 2 L_3 t_f N_f L_1 \quad (A-25)$$

$$A_{total} = A_p + A_f \quad (A-26)$$

$$N_t = \frac{L_3 \left(\frac{L_2}{P_t} + 1 \right)}{2 p_t} + \left(\frac{L_3}{P_t} - 1 \right) \frac{L_2 / P_t - 1}{2} \quad (A-27)$$

Where A_p and A_f are plate and fin surfaces respectively. $L_{1,2,3}$, P_t , t and d are showed in Fig. A-1.

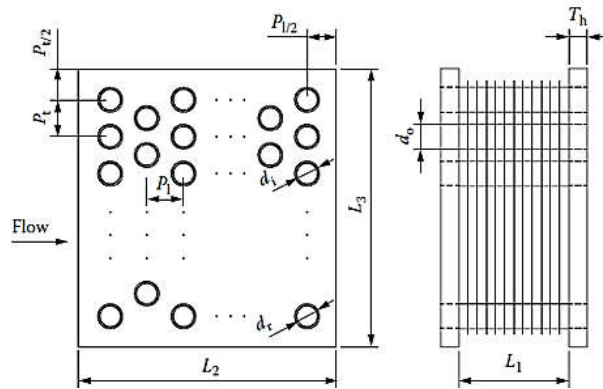


Fig A-1. heat exchanger schematic

heat transfer coefficient

$$UA = \frac{1}{\left(\frac{1}{h_{ac} A_a} + \frac{1}{h_w A_w} \right)} \quad (A-28)$$

$$h_w = 319 + 15.79 (T_{w,ave})^{0.8} \quad (A-29)$$

$$h_{ac} A_a = \left(\frac{1}{h_a e_f A_a} + \frac{\ln \left(\frac{d_o}{d_i} \right)}{2 k_t \pi L_t n_{tb} n_b} \right) \quad (A-30)$$

$$h_a = J_{uncoated} Re_O \cdot Pr^{\frac{1}{3}} \quad (A-31)$$

$$J_{uncoated} = 0.2476 Re_O^{-0.209} \left(\frac{S_{f,Heller}}{d_{o,Heller}} \right)^{0.4325} \left(\frac{S_{f,Heller} N_{row}}{d_{o,Heller}} \right)^{-0.3792} \quad (A-32)$$

Fin relations

$$e_f = 1 - \frac{A_f}{A_a} (1 - \eta_f) \quad (A-33)$$

$$\eta_f = \frac{\tanh\left(\frac{bd_r \Phi}{2}\right)}{\frac{bd_r \Phi}{2}} \quad (A-34)$$

$$\Phi = \left(d_f / d_r - 1 \right) \left[1 + 0.25 \ln\left(d_f / d_r \right) \right] \text{ and } b = \left(\frac{2h_a}{t_f k_f} \right)^{0.5} \quad (A-35)$$

Where A_w , A_a are the total surface of water side and air side, h_w and h_{ac} are the heat transfer coefficient of water side and air side, e_f is the effectiveness of the finned surface, η_f is the fin efficiency, d and t are the diameter and thickness [30], [31]. The relations for deluged mode are reported in ref. [30], [31].

A.5.) Solar field

energy balance for the solar collector absorber tube:

$$\dot{q}_{solar} = \dot{q}_{Rad} + \dot{q}_{conv} + \dot{q}_{cond} + \dot{q}_{cond, bracket} \quad (A-36)$$

the convective heat transfer to the working fluid is:

$$\dot{q}_{conv} = h_{HTF} D_{in} \pi (T_w - T_{flow}) \quad (A-37)$$

$$h_{HTF} = Nu_{D_{in}} \frac{k}{D_{in}} \quad (A-38)$$

Nusselt number for calculating the turbulent flow:

$$Nu_{D_2} = \frac{f/8 (Re-1000) Pr}{1 + 12.7 \sqrt{f/8} \left(Pr^{\frac{2}{3}} - 1 \right)} \quad (A-39)$$

$$f = \left(1.82 \log\left(Re_{D_{in}} \right) - 1.64 \right)^{-2} \quad (A-40)$$

conductive heat transfer equation from the absorber tube:

$$q_{cond} = 2\pi k (T_w - T_{flow}) / \ln(D_{out} / D_{in}) \quad (A-41)$$

$$k = (0.0153) k_0 + 14.775 \quad (A-42)$$

Convection heat transfer from tube outer surface into the ambient:

$$q_{conv} = h\pi D_{out} (T_w - T_{amb}) \quad (A-43)$$

$$Nu_{D_{out}} = \left\{ 0.06 + \frac{0.387 Ra_{D_{out}}^{1/6}}{\left[1 + (0.559/Pr)^{9/16} \right]^{8/27}} \right\}^2 \quad (A-44)$$

$$Ra_{D_{out}} = \frac{g\beta(T_w - T_{amb})D_{out}^3}{(\alpha\nu)} \quad (A-45)$$

$$\beta = \frac{1}{T_{ave}} \quad (A-46)$$

Radiation amount between tube surface and the ambient:

$$q_{Rad} = A_1 F_{sur} (J_1 - J_{sur}) \quad (A-47)$$

$$J_1 = E_{b1} - q \frac{(1 - \epsilon_1)}{\epsilon_1 \pi D} \quad (A-48)$$

$$J_{sur} = \sigma T_{sky}^4 \quad (A-49)$$

$$F_{sur} = \frac{\theta}{360} \quad (A-50)$$

Where q_{solar} , q_{rad} , q_{conv} , q_{cond} , $q_{cond,bracket}$, $q_{HeatLoss}$ are respectively the solar radiation energy, radiation heat transfer losses, convection and conduction heat transfer and heat transfer losses from the brackets and the losses of one element. f and Pr are friction coefficient for inner surface of the tubes and Prandtl number for the working fluid respectively. k is the thermal conductivity of the absorber tube. β is volumetric thermal expansion coefficient, ν is kinematic viscosity, Ra is Rayleigh number. All are considered in the mean temperature of tube surface (T_w) and ambient (T_{amb}), T_{ave} . σ , ϵ , θ and T_{sky} are respectively Stefan Boltzmann constant, emissivity, collector angle with the sky and the sky temperature [33], [34].